Journal of Volcanology and Geothermal Research 185 (2009) 290–297

Contents lists available at ScienceDirect

Journal of Volcanology and Geothermal Research

journal homepage: www.elsevier.com/locate/jvolgeores

Tephra deposition on glaciers and ice sheets on Mars: Influence on ice survival, debris content and flow behavior

L. Wilson [a,b,*], J.W. Head [b]

[a] Environmental Science Department, Lancaster University, Lancaster LA1 4YQ, UK
[b] Geological Sciences Department, Brown University, Providence RI 02912, USA

ARTICLE INFO

Article history:
Received 30 April 2008
Accepted 9 October 2008
Available online 18 October 2008

Keywords:
Mars
glacier
volcano
tephra

ABSTRACT

We examine the consequences of pyroclastic deposits being emplaced onto ice layers on Mars, both those in the polar caps and those forming glaciers on the flanks of some of the large shield volcanoes. We show that layers of pyroclasts greater than a few meters in thickness, whether emplaced cold (as fall deposits) or hot (as pyroclastic density current deposits) act almost exclusively to protect ice layers beneath them from sublimation, irrespective of whether they are emplaced at high or low elevations or high or low latitudes. Layers less than about 2 m thick, on the other hand, can cause significant ice loss by raising the surface temperature due to their low albedo and then transmitting that increased temperature to the underlying ice, especially on a diurnal time scale. This can have a significant bearing on the emplacement history of polar water ice and on the survival time of glacial ice on shield volcano flanks. A key factor in the latter case is the timing of the episodic volcanic activity relative to the cycles of climate change driven by Mars' obliquity and eccentricity variations.

1. Introduction

Water ice deposits, averaging ~3 km in thickness, currently exist at the poles of Mars (Smith et al., 1999; Phillips et al., 2007), and water ice is present at depths less than 1 m in the crust in both hemispheres at latitudes greater than ~50° (Boynton et al., 2002; Mellon et al., 2004). It has recently been realised that water ice has also been present as glaciers on the flanks of a number of tropical volcanic mountains, especially those in the Tharsis province (Head and Marchant, 2003; Shean et al., 2005, 2007; Milkovich et al., 2006; Kadish et al., 2008) (Fig. 1), and that the spatial extents of the glacial deposits on these mountains, which are currently as large as 17,000 km^2, have varied significantly with time. Changes in the spatial extents and thicknesses of tropical mountain glaciers on the Tharsis volcanoes, and of glacial ice deposits at other latitudes (e.g., Head et al., 2006a,b), are influenced by temperature changes on a variety of time scales, the most important of which are controlled by changes in the obliquity of Mars' spin axis and the eccentricity of its orbit around the Sun. Three time scales are prominent, ~100 ka, 2 Ma and 15 Ma (Laskar et al., 2002). However, these climatic controls may be modified by any other process that affects the temperature or reflectivity of an ice surface. The purpose of this paper is to explore the consequences of the deposition of volcanic fall and flow deposits onto glacial and polar ice layers on Mars.

Volcanic eruptions on Mars have taken place over protracted periods; the Tharsis volcanoes have been built up over time periods estimated to be of order 1 to 2 Ga (Schaber et al., 1978; Hodges and Moore, 1994). Dividing their volumes, which lie within a factor of 3 of 1.5×10^6 km^3 (Wilson et al., 2001), by their ages gives a mean magma supply rate of ~0.05 m^3 s^{-1}, with a range that also spans a factor of at least 3. The most recent eruptions on these volcanoes are not easy to date, but impact crater counts on the floors of their calderas suggest that eruptions have taken place within the last 25–50 Ma (Neukum et al., 2004). All of the Tharsis volcanoes have multiple summit calderas, implying that each one has developed at least several magma chambers during its lifetime (e.g., Scott and Wilson, 2000). Thermal constraints (Wilson et al., 2001) mean that the initiation of a new magma reservoir requires a high magma supply rate (~150 m^3 s^{-1}) for many weeks; to maintain the reservoir requires an input of ~3 m^3 s^{-1} (again with a range encompassing a factor of ~3) throughout its active lifetime. To allow an existing reservoir to cool and solidify, so that a subsequent reservoir can be constructed at a location offset from that of its predecessor, requires the absence of significant magma supply for at least several tens of Ma.

The simplest way to reconcile all of these requirements is to assume that each of these volcanoes is (intermittently) active for ~1 Ma and then dormant for ~100 Ma, this long-term cycle being repeated throughout most of the lifetime of the volcano (Wilson et al., 2001). Thus for a 1.5 Ga volcano lifetime, 15 such cycles would be required, with 100,000 km^3 of magma being supplied to the summit

* Corresponding author. Environmental Science Department, Lancaster University, Lancaster LA1 4YQ, UK. Tel.: +44 1524 593889; fax: +44 1524 593985.
E-mail addresses: L.Wilson@lancaster.ac.uk (L. Wilson), James_Head@Brown.edu (J.W. Head).

0377-0273/$ – see front matter © 2008 Elsevier B.V. All rights reserved.
doi:10.1016/j.jvolgeores.2008.10.003

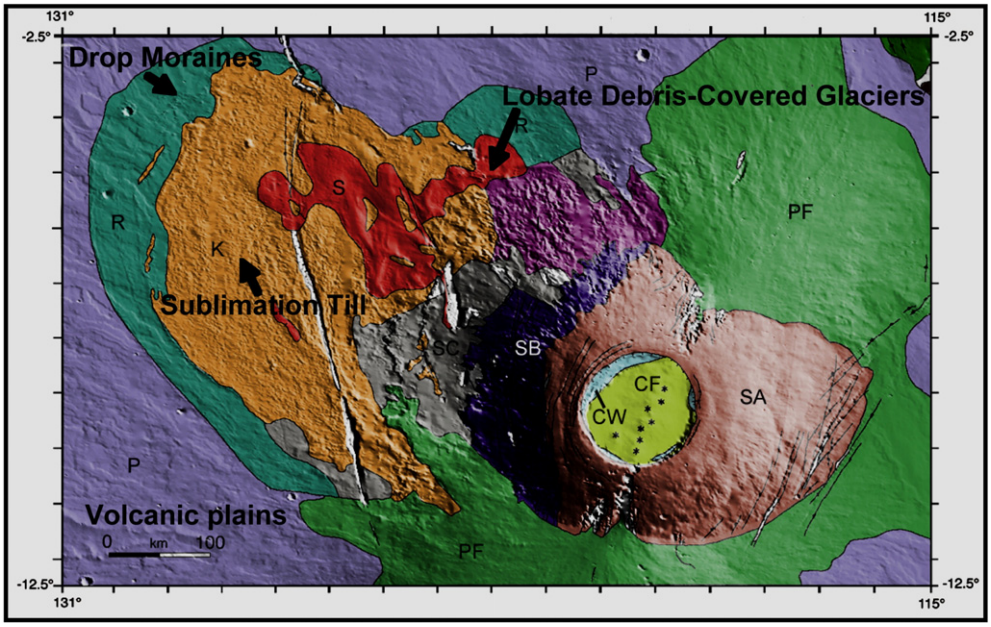

Fig. 1. Current extent of deposits interpreted as drop moraines, sublimation till, and smooth, debris-covered glacial ice on Arsia Mons volcano, Mars. Modified from Head and Marchant (2003).

reservoir per cycle. This volume would have to be erupted in each of the ~1 Ma active periods. By analogy with shield volcanoes on Earth, eruptive activity may be dominated by short-term cycles of reservoir inflation and eruption (or intrusion) in which at most ~1% of the reservoir magma is released per cycle (Blake, 1981). If so, then a 30 km diameter reservoir, typical of those implied by the calderas visible on martian shield volcanoes today, would have an event erupting or intruding ~71 km^3 of magma on average every ~710 years.

To illustrate the possible effects of this kind of eruption we simulate below the dispersal of 100 km^3 of magma erupted in a single event, noting that ~1000 such eruptions may occur at ~1000 year intervals during any 1 Ma active phase of the volcano. We also simulate the presumably much rarer events in which caldera subsidence occurs as a result of the rapid withdrawal of an unusually large volume of magma. Noting that the calderas of the martian shield volcanoes have depths up to ~1 km, implying that a 30 km diameter reservoir underlying such a caldera could erupt as much as 7000 km^3 of magma, we conservatively simulate the eruption of 1000 km^3 of magma in a single event. Given that the low atmospheric pressure on Mars encourages explosive activity in magmas with much smaller volatile contents than those common on Earth (Wilson and Head, 1994), there are strong reasons for anticipating that a mixture of effusive and explosive deposits form the bodies of these volcanoes (Head and Wilson, 1998; Wilson et al., 1998). We focus here on explosive eruptions because, as we show in the next section, pyroclasts produced in such eruptions are likely to blanket much greater areas than are observed to be covered by lava flows.

2. Tephra production and injection into the atmosphere

The expectation that volcanic eruptions on Mars are inherently more likely to be explosive than eruptions of similar magmas on Earth because of the lower atmospheric pressure arises from two effects (Wilson and Head, 1994). First, available volatiles, all of which have solubilities that are pressure-dependent, exsolve to a greater degree; second, all of the gas bubbles formed from the volatiles released undergo a greater amount of expansion than on Earth. The combined effect on Mars is likely to be a greater degree of fragmentation of the magma, with the size of the largest pyroclast formed being much smaller than on Earth: Wilson and Head (1994) estimated a maximum grain size of a few mm, and for convenience here we adopt the value ~5.6 mm, i.e. −2.5 phi units. The size of the smallest pyroclast is likely to be controlled by the size of the smallest bubble that can nucleate, ~20 μm (Sparks, 1978), and we adopt ~22 μm, i.e. +5.5 phi units. Thus the net effect is to produce a smaller range of grain sizes than on Earth and a smaller median size. These findings appear to be consistent with the sizes of the pyroclasts resulting from eruptions into a hard vacuum on the Moon, where the maximum sizes of the volcanic glass beads found in the lunar regolith are ~1 mm (Weitz et al., 1998).

A second consequence of the low atmospheric pressure and enhanced gas expansion on Mars is higher exit velocities than on Earth in the ejected mixture of gas and pyroclasts for a given total magma volatile content (Wilson and Head, 1994). As a result the jet of gas and pyroclasts that emerges from the vent is able to entrain the surrounding atmospheric gas more efficiently. Furthermore, the small sizes of the pyroclasts mean that they remain locked to the gas motion (because they have small ratios of mass to cross-sectional area and hence small terminal fall velocities relative to the gas), and also that they can release their heat to the entrained gas efficiently (because the timescale for extracting the heat is proportional to the square of the radius). The net result is to maximize the thermal buoyancy of the plume formed from the mixing of atmosphere and volcanic materials and hence to maximize the rise height of that plume for a given mass eruption rate from the vent. Indeed, the great efficiency of entrainment of the pyroclasts into the gas flow means that eruptions which would shed a large proportional of their coarse pyroclasts not far above the vent on Earth, forming a lava fountain (often called fire fountain), will instead form a high convecting plume on Mars of the kind more commonly associated with plinian eruptions on Earth (Wilson and Head, 1994).

To a good approximation, the maximum heights of eruption plumes are proportional to the fourth root of the erupted mass flux (e.g., Wilson et al., 1978). However, this relationship is only valid as long as the atmospheric and volcanic gases obey the normal gas laws. At sufficiently great heights above the surface on Mars, the gas density becomes so low that the mean free path of molecules becomes very large, comparable to the sizes of pyroclasts, and interactions take place in the Knudsen regime (Glaze and Baloga, 2002). Both the support of clasts and the entrainment process then become very inefficient and, as a result, eruption plumes are not likely to be able to rise to heights

Table 1
Size distribution proposed for pyroclasts on Mars, expressed as the fraction of the total erupted mass in a given half-phi size range.

Size range in mm	Size range, ϕ units	Mass fraction
4.0000 to 5.6569	−2.0 to −2.5	0.00800
2.8284 to 4.0000	−1.5 to −2.0	0.04700
2.0000 to 2.8284	−1.0 to −1.5	0.06399
1.4142 to 2.0000	−0.5 to −1.0	0.06900
1.0000 to 1.4142	0.0 to −0.5	0.07200
0.7071 to 1.0000	0.5 to 0.0	0.07400
0.5000 to 0.7071	1.0 to 0.5	0.07700
0.3536 to 0.5000	1.5 to 1.0	0.07800
0.2500 to 0.3536	2.0 to 1.5	0.07700
0.1768 to 0.2500	2.5 to 2.0	0.07900
0.1250 to 0.1768	3.0 to 2.5	0.10600
0.0884 to 0.1250	3.5 to 3.0	0.10600
0.0625 to 0.0884	4.0 to 3.5	0.06500
0.0442 to 0.0625	4.5 to 4.0	0.04000
0.0312 to 0.0442	5.0 to 4.5	0.02699
0.0221 to 0.0312	5.5 to 5.0	0.01100

much greater than ~20 km on Mars (Glaze and Baloga, 2002; Wilson and Head, 2007a). The mass eruption rates required to reach this height are so small (only ~5000 kg s^{-1}, corresponding to a dense rock equivalent volume eruption rate of ~2 m^3 s^{-1}) that a very large proportion of all eruptions on Mars should produce eruption plumes reaching, but not greatly exceeding, a height of 20 km. The widths of the plumes at this height cannot be easily predicted because the theoretical models used to simulate martian explosive eruptions no longer apply near the 20 km level. However, the modeling of terrestrial eruptions (e.g., Carey and Sparks, 1986; Sparks, 1986; Wilson and Walker, 1987) suggests that the plume radius will be about half of the plume height near the plume top, implying that the bulk of the pyroclasts are released from a circular region ~10 km in radius.

There is an addendum to the above result: for an eruption in which the exsolved magma volatile content is greater than ~1.7 mass % and the mass flux is greater than ~6×10^7 kg s^{-1}, the jet formed at the vent can effectively punch through the atmosphere with minimal interaction and thus form an inertial or "umbrella"-type plume closely akin to the kind observed on Io (Wilson and Head, 2007a). Pyroclasts may then travel to heights above the surface much greater than 20 km, but they will very quickly (1 to 3 min) fall back ballistically under gravity until they encounter the drag effects of the atmosphere as they descend through the ~20 km level. They will then fall to the ground with much the same duration of travel as if they had been transported to the 20 km level by an eruption with a much smaller mass eruption rate. The main difference is that their excursion out of, and back into, the lower atmosphere will mean that they start their descent from the 20 km level at much greater radial distances (~40–60 km) from the vent (Wilson and Head, 2007a). The amount by which this affects their total travel distance then depends on the mean wind speed and their sizes. In a typical martian wind profile (Moudden and McConnell, 2005), where the speed increases steadily to values of ~40 m s^{-1} at ~20 km, large (~2 mm) clasts will fall quickly (at ~50 m s^{-1}) and travel only a further 10 km from their re-entry point, so the "umbrella" effect will significantly influence their dispersal. In contrast, the smallest (20 μm) clasts will fall extremely slowly (at ~0.01 m s^{-1}) and in principle could travel 60,000 km, about 3 times around the planet. Clearly for these small clasts the details of how they reach the 20 km high re-entry point are irrelevant. For the intermediate case of 200 μm clasts the fall speed from 20 km averages ~1 m s^{-1} and in the distance traveled is ~600 km, so in this case too the details of what happens in the vicinity of the vent are of minimal importance.

3. Pyroclast dispersal and deposit thicknesses

The above finding, that most explosive eruptions on Mars will transport the bulk of their erupted pyroclasts to heights close to 20 km and release them from this height in a region that may extend horizontally from between ~10 and ~50 km from the vent, greatly simplifies modeling their dispersal. The grain size determines the fall speed and hence the travel distance in a typical wind profile after release into the lower atmosphere, and so the total grain size distribution released at the vent will be the control on the amount of material that falls at a given distance, and hence the local thickness of the deposit. There are no grain size distribution determinations for any of the explosive eruption deposits on Mars suggested by image analysis of volcano morphology (e.g. Edgett et al., 1997; Mouginis-Mark et al., 1982, 1988), and the suggested identification of mm-sized lapilli in strata examined by the Mars Exploration Rover Spirit in Gusev crater (Cabrol, 2006; Rice et al., 2006) does not provide a significant part of a size distribution.

We described above how estimates can be made of the largest and smallest grain sizes. To obtain a grain size distribution function for Mars we take a typical distribution found for very explosive eruptions on Earth and scale it to our predicted maximum and minimum martian grain sizes. Total grain size distributions are hard to measure for ancient explosive eruptions on Earth because of the difficulty of identifying thin, fine-grained, poorly-preserved distal deposits in the geological record, but data from some modern eruptions are summarized by Wilson (1999). Of these, the one with the most thoroughly fragmented magma is the Askja 1875 eruption, and we use grain size data for it, taken from Wilson (1999), as the basis for the proposed Martian grain size distribution (Table 1).

Deposit thickness is predicted as follows. We assume that erupted clasts of all sizes are carried to the 20 km height and release them at a chosen radial distance from the vent (in the range 10 and ~50 km identified above). We then use the equations given by Wilson and Head (2007a) for determining terminal fall velocities of clasts of a given density in a standard martian atmosphere to obtain the fall speed for each particle size as a function of height above the ground. The lateral displacement of each particle size as it falls is tracked via the atmospheric wind model of Moudden and McConnell (2005) and integrated until the clast size reaches the ground. If no other action were taken this process would lead to a one-to-one relationship between clast size (of a given density, in this case 1500 kg m^{-3}, a plausible pyroclast density) and travel distance, and this relationship is shown in Fig. 2. However, turbulence in a planetary atmosphere causes significant dispersion of falling particles, and we allow for this by smearing out the unique travel distance into a distribution that is centered at a chosen fraction α of the nominal range and has a standard deviation that is

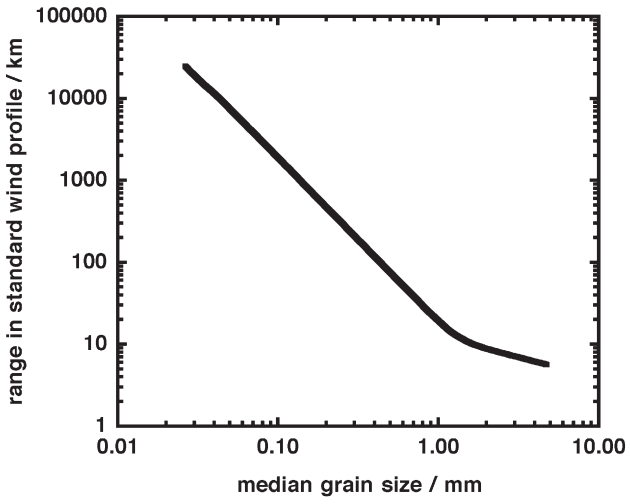

Fig. 2. The relationship between grain size and down-wind range in a standard atmosphere and wind profile on Mars if no lateral spreading of particles occurs as they fall.

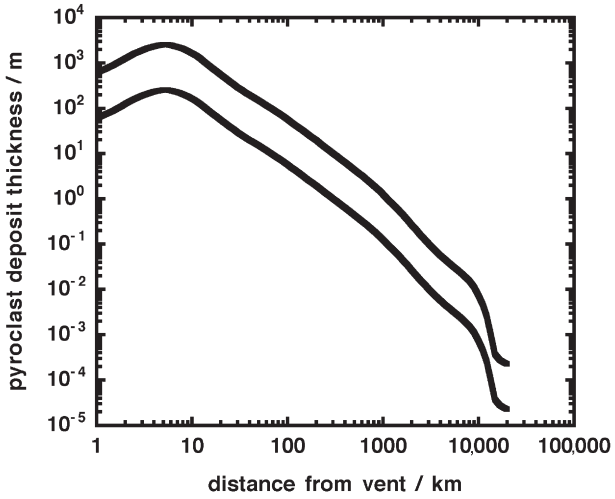

Fig. 3. Predicted variation of pyroclastic fall deposit thickness with distance from vent on Mars for particles released from an eruption column, or injected into the lower atmosphere from above, at a height of 20 km above the ground. Curves are labelled with the two values of the total erupted magma volume modelled, 100 and 1000 km^3.

some other chosen fraction β of the nominal range. For illustration, values of $\alpha = 0.6$ and $\beta = 0.6$ are chosen; the exact values do not alter the overall distribution of material greatly (the main effect is that increasing α and β increases the maximum distance that can be reached by the finest material), but they do alter the size distribution somewhat at any given locality. This is not important in the present study as we are only concerned with the thickness of the deposit. The total grain size distribution of Table 1 is used, together with the total erupted volume, to obtain the total volume of a given grain size that reaches the ground, and this volume is distributed with distance from the vent in accordance with the smearing function into bins defining finite range increments. The thickness of the deposit in each bin is found by dividing the volume in the bin by the along-range bin length and the width of the deposit. To find the latter, it is assumed that the eruption cloud spreads laterally as it travels downwind in the same way that a thermal plume spreads when rising vertically (Morton et al., 1956), so that the ratio of width increment to down-wind distance increment is 1/8. This spreading rate is comparable to values found in the simulation of volcanic plumes on Earth (e.g. Turner and Hurst, 2001), and the dispersal pattern produced is similar to that from a more sophisticated model of the atmospheric transport (Kerber et al., 2008).

Fig. 3 shows the resulting deposit thickness for the two cases defined in the previous section by the arguments about likely erupted volumes: 100 km^3 and 1000 km^3. If the erupted volume is 100 km^3 it would be expected that the deposit thickness within ~10 km of the vent would be ~100–300 m, thinning to ~1 m at 200–300 km range (i.e. at the edge of the main shield in the case of the Tharsis volcanoes) and to 1 cm at 2000–3000 km distance. The thickness would only decrease to less than 1 mm half way around the planet. For the larger (but probably much rarer) 1000 km^3 volume, the thickness within 10 km of the vent could be more than 1000 m, and would still be ~200 m at the edge of the main shield. The thickness would decrease to ~1 cm half way around the planet and the finest material would be blown completely around the planet. We now consider the potential effects of the deposition of these pyroclast layers if they fall onto glacial or polar ice deposits.

4. Thermal consequences of pyroclast deposition

4.1. Basic considerations

The largest clasts expected to be erupted, ~5 mm in size, require ~230 s to descend from a height of ~20 km in the standard Mars atmosphere (Wilson and Head, 2007a). The time τ required for a spherical clast of radius a to equilibrate in temperature with its surroundings is given by $a = \sim 1.4\ (\kappa\, t)^{1/2}$ (Carslaw and Jaeger, 1947, p. 201) where κ is the thermal diffusivity, $\sim 7 \times 10^{-7}$ m^2 s^{-1} for silicates, and so with a equal to 2.5 mm, τ is 6 to 7 s. Thus, other than perhaps extremely close to the vent, all pyroclasts in fall deposits on Mars are likely to be at ambient atmospheric temperature on reaching the ground. This does not mean that they will have no effect on the stability of surface ice, however. Pyroclasts are likely to have a significantly lower albedo than ice, and will therefore absorb solar insolation more efficiently than ice, raising the surface temperature. If this temperature increase is communicated by conduction through the pyroclast layer to the ice below, it will raise the temperature, and hence the vapor pressure, of the ice, potentially increasing the sublimation rate. However, the presence of a layer of pyroclasts on top of ice inhibits sublimation of the ice into the atmosphere by introducing a tortuous pathway that must be negotiated by H_2O molecules before they can escape. Both of these processes are time and layer-thickness dependent, and we next consider their relative importance.

The warming effect can be quantified by considering the balance between the incoming solar heat flux per unit area, S, and the heat flux per unit area radiated by the surface, $R = \varepsilon\, \sigma\, T^4$, where ε is the emissivity, σ is the Stephan–Boltzman constant, and T is the absolute surface temperature. Clearly, at equilibrium the surface temperature is inversely proportional to the fourth root of the emissivity. The albedoes of the polar ice caps on Mars range up to 0.4 at the North pole (Kieffer and Titus, 2001) and 0.7 at the South pole (James et al., 2005), whereas mafic silicates have albedoes as small as 0.1 (Farrand and Singer, 1992). The corresponding emissivities are 0.3–0.6 and 0.9, and so the effect of emplacing a layer of pyroclasts will be to increase the surface temperature by a factor between $(0.9/0.3)^{1/4} = \sim 1.31$ and $(0.9/0.6)^{1/4} = \sim 1.11$. Fig. 4 shows the relationship between temperatures before and after emplacement of a low-albedo mafic pyroclast layer on bright ice. A surface previously at the mean martian surface temperature of ~210 K will have its temperature raised to ~276 K, about 3° above the melting point of ice. In polar and high-altitude locations where the temperature is very much less than the planetary mean (perhaps as low as ~130 K — Mellon et al., 2004), the temperature will not be raised above the melting point; but the sublimation rate of H_2O molecules (whether from a solid or a liquid surface) is an extremely strong function of the temperature, and there may still be a major effect on the long-term ice stability. At lower latitudes, where ice with a temperature significantly greater than the

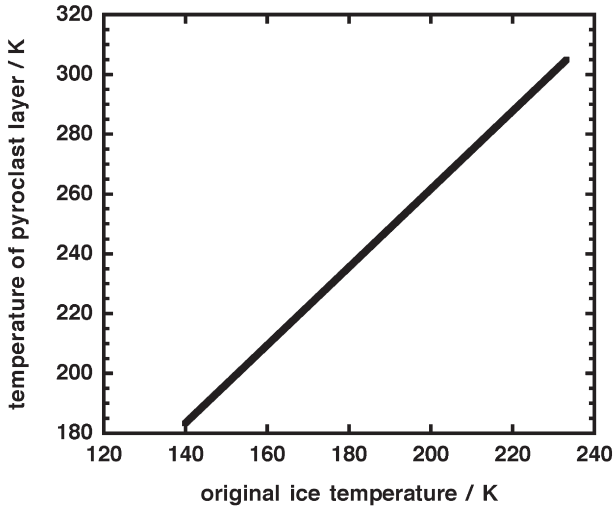

Fig. 4. Relationship between the temperature of an icy surface and temperature of the surface of a low-albedo mafic pyroclast layer emplaced on top of it under the same solar illumination conditions.

Table 2
Values of the depth of penetration of a thermal wave in time t, $\sim 2.32\,(\kappa t)^{1/2}$, for various time scales of periodic temperature change relevant to the Mars surface. An average value of $\kappa = 7\times10^{-7}$ m^2 s^{-1} is used for the thermal diffusivity.

Time frame	Time in seconds	Penetration depth
Mars day	8.86×10^4	0.58 m
Mars year	5.94×10^7	15 m
1 century	3.16×10^9	109 m
1 ka	3.16×10^{10}	345 m
10 ka	3.16×10^{11}	1.1 km
100 ka	3.16×10^{12}	3.5 km
2 Ma	6.31×10^{13}	15 km
15 Ma	3.16×10^{14}	42 km

planetary mean might be present (Mellon et al., 2004), the temperature could in theory be raised well above the ice melting point. However, thermal observations from orbit (Kieffer et al., 1976a, b; Haberle et al., 2001; Grassi et al., 2005) suggest that no significant part of the martian surface is ever hotter than ~30 °C, and so we adopt 300 K as a realistic upper limit to the temperatures to be considered. We note in passing that both Viking (Kieffer et al., 1976a,b) and Mars Express (Grassi et al., 2005) data show that the summits and upper flanks of the large Tharsis shield volcanoes can attain daytime temperatures several degrees above 273 K. Given that the atmospheric pressure at the summits is ~130 Pa, only a fraction of the ~610 Pa vapor pressure of ice at 273 K, it is clear that long-term ice survival without a protective cover of some kind is not to be expected and, indeed, Mars Odyssey gamma ray and neutron spectrometer data show evidence for the presence of water ice within about 1 m of the surface on the lower north-west flanks of the Tharsis shields but not in the summit areas (Elphic et al., 2004).

Raising the surface temperature of a layer of pyroclasts to a value above the melting point of ice does not mean that ice buried beneath the pyroclasts will melt immediately. The response of the ice depends on the time taken by the heat input at the surface to penetrate to the ice, and hence on the deposit thickness. Solar heat inputs to the surface of Mars vary on two short time scales, the Mars solar day (1 sol = 24.624 h) and one Mars year (=686.98 days), and on three longer time scales, those of the obliquity and eccentricity cycles (Laskar et al., 2004), ~100 ka, 2 Ma and 15 Ma. Table 2 shows the depth of penetration beneath the surface of a thermal wave driven by each of these five periodicities. Temperature fluctuations due to each of these driving periodicities will be significant down to depths 2 to 3 times greater than the values given. Clearly, for pyroclast layers less than about 2 m thick, buried ice will respond to the diurnal heating cycle. For layer thicknesses in the ~2 m to ~30 m range, the diurnal variations will be largely ignored but the annual cycle will be felt. Finally, all deposits will be influenced by all three of the long-term climate variation periodicities.

If the temperature of the ice at the bottom of the pyroclast layer rises to a value such that the temperature-dependent vapor pressure exceeds the local atmospheric pressure, molecules will begin to diffuse upward between the pyroclasts and be lost to the atmosphere at the surface. Their rate of loss depends on the porosity, pathway tortuosity and thickness of the pyroclast layer. Both the porosity and the tortuosity may be progressively changed from their initial values by the presence of ice temporarily deposited in pore spaces as molecules migrate. This problem has been treated for loss of ice from beneath a dust layer on comets (Fanale and Salvail, 1984) and on Mars' satellite Phobos (Fanale and Salvail, 1990). The mass flux of H_2O lost per unit area of the deposit, q_m, is given by

$$q_m = \frac{4}{9}\left[\frac{2M}{\pi QT}\right]^{1/2}\frac{fr(P_T - P_A)}{\tau^2 h} \quad (1)$$

where M is the molecular mass of water (18.02 kg kmol^{-1}), Q is the universal gas constant (8.314 kJ kmol^{-1} K^{-1}), T is the ice temperature, f is the bulk porosity of the pyroclast layer, r is the typical size of the pathways between pyroclasts, P_T is the vapor pressure of the ice at temperature T, P_A is the local atmospheric pressure, τ is the tortuosity of the pyroclast layer, and h is the layer thickness. A likely value for τ is 5 (Fanale and Salvail, 1990). To estimate f we note that we expect thorough disruption of the magma so that individual pyroclasts may not be very vesicular; close packing of the likely irregular particles will produce a porosity of ~35% (Latham et al., 2002). The requirement that the vapor pressure of the ice must exceed the local atmospheric pressure for sublimation to occur sets a lower limit to the ice temperature that needs to be considered. The greatest heights of volcano summits above the pressure datum on Mars are ~20 km, very close to two scales heights of the martian atmosphere. Thus for a mean surface pressure of ~700 Pa, the pressure at the top of the highest volcano is ~100 Pa, and this is the vapor pressure of ice at ~−20 °C, i.e. 253 K. We therefore identify this as the lowest temperature at which significant ice sublimation could ever occur in the absence of wind-driven loss (Wallace and Sagan, 1979), and of course winds will have no effect beneath a protective layer of pyroclasts.

Eq. (1) has been used to obtain water molecule mass fluxes for a range of ice or water temperatures and atmospheric pressures under a range of pyroclastic blanket thicknesses. The temperature range is taken as 253 to 300 K on the basis of the above arguments, and the pressure range is 700 to 100 Pa, covering all volcano summits and flanks. The water molecule mass fluxes are converted to ice thickness reduction rates by dividing the mass flux per unit area by the ice density. Multiplication of this by any given time interval yields the actual ice thickness loss during that time period.

4.2. Thin pyroclast deposits responding to diurnal temperature changes

Ice buried beneath pyroclast deposits with thicknesses less than ~2 m will respond to diurnal temperatures variations (Table 2). Pyroclast deposits with thicknesses in this range will be located at distances greater than ~200 km from the vent in the case of 100 km^3 eruptions and greater than ~800 km for the rarer 1000 km^3 events. Thus we are mainly concerned here with thin deposits that either fall on polar ice or on one volcano as a result of an eruption on some other volcano. Table 3 shows the depth of ice lost from an ice layer as a function of the ambient atmospheric pressure and the overlying pyroclast layer thickness in one sol (martian day). Note that ice is only lost during that part of the sol when the temperature at the base of the pyroclast layer is such that the ice vapor pressure exceeds the local atmospheric pressure. For the temperature range modeled, 140 to 300 K, this period is ~12% of the sol.

At the polar caps the atmospheric pressure is in the 600–800 Pa range and the maximum temperature is ~240 K (Haberle et al., 2001). With the maximum amount of heating (which Fig. 4 shows to be ~70 K) by the warming effect of a 0.1 m thick pyroclast layer, several hundred micrometers of ice could be lost each sol, and during the ~330 sol-long summer months the total loss could exceed 0.1 m. Modelling by Laskar et al. (2002) suggests that a thickness of only ~0.5 mm of water ice is deposited on each polar cap during each martian winter under present climatic conditions. Thus volcanic fall

Table 3
Water ice loss rates in micrometers per sol from an ice layer buried beneath a pyroclast layer for a range of atmospheric pressures covering martian volcanic flanks from the base to the summit and a range of pyroclast layer thicknesses.

Atmospheric pressure in Pa	Pyroclast layer thickness in meters				
	0.1	0.3	0.7	1	2
100	1183	394	169	118	59
300	922	307	132	92	46
500	717	239	102	72	36
700	582	194	83	58	29

events could seriously disturb the long-term polar ice recycling due to obliquity and eccentricity changes. These issues merit more detailed investigation.

The situation is equally complex on the flanks of volcanoes. The time scale for glacier formation is the 100 ka obliquity variation, and measurements indicate that as much as 3 km of ice can accumulate (Dickson et al., 2008) on the Tharsis shield volcanoes. If this thickness accumulates over one half of 1 cycle, 50 ka, the average accretion rate is ~170 μm per sol. The loss rate from an ice layer due to an overlying pyroclast layer can lie anywhere in the range 30 to 1200 μm per sol, with loss rates decreasing away from the summit and decreasing with increasing pyroclast layer thicknesses (Table 3). There are two extreme cases to consider.

First, assume that near the start of an orbital ice accumulation cycle ice deposition starts between the 500 Pa (lower flanks) and 100 Pa (summit) levels on a Tharsis volcano at the above average rate of 170 μm per sol. After the typical repose time of 1000 years an eruption occurs on a distant volcano that is in the 1 Ma active part of its 100 Ma activity cycle. This eruption deposits 0.3 m of ash on the accumulating ice deposit, which in 1000 years has accumulated to a thickness of 62 m. If the eruption ends early in the daylight hours, diurnal heating of the pyroclast layer rapidly penetrates the 0.3 m thick ash layer and ice beneath it begins to be lost at rates of 239, 307 and 394 μm per sol at the lower flank, upper flank and summit levels. If this loss rate continued indefinitely, all of the ice would be lost at these levels in 710, 553 and 431 years, respectively. However, on average ~150 μm of fresh ice will be deposited onto the top of the pyroclast layer during the ~88% of the next sol that the surface temperature is below 273 K. Given that we expect the grain sizes in the pyroclast layer to be at most 5 mm, i.e. 500 μm, this single night's ice deposit should be enough to completely veneer the uppermost surface and drastically increase its albedo, thus destroying the potential heating process. In practice, the ice build-up rate is not likely to be constant at the average rate but is likely to be episodic depending on the sol-to-sol weather patterns. However, as long as one significant snow fall occurs on a time scale much less than a few centuries, most of the ice layer will survive. We therefore infer that eruptions taking place during an ice-accumulation period will not significantly interfere with the accumulation. Instead, they will simply interleave pyroclast layers with ice layers.

Now consider the case where an eruption occurs after an orbital ice accumulation cycle has finished. An ice layer 3 km thick is assumed to be present, onto which, as before, 0.3 m of ash is deposited by a distant eruption. Now no new ice is deposited overnight to interfere with the diurnal heating cycle. The ice loss rates from beneath the pyroclast layer will be those given above, 239, 307 and 394 μm per sol on the lower flanks, upper flanks and summit of the volcano, respectively. During the on-average 1000 years before the next eruption of the volcano forming the first pyroclast layer, the 3 km ice layer will have thinned by 87, 112 and 144 m, respectively, at the three locations. Assume that the next eruption deposits the same thickness of ash. The ice loss rates from beneath the now 0.6 m thick layer will be less than before, specifically 120, 154 and 197 μm per sol, and the ice thickness reductions during a subsequent 1000 year interval would be 44, 56 and 72 m, respectively. Assume that after this further 1000 years a third similar eruption occurs. The ice loss rates under the resulting 0.9 m thick ash layer will be 80, 102 and 131 μm per sol, and the ice thickness reductions will be 29, 37 and 48 m. Potentially this pattern can continue for a total of 50 eruptions at 1000 year intervals during the no-ice-accumulation part of the 100 ka obliquity cycle. If it does so, repetition of the above calculation shows that the total ice thickness removed from the lower flanks, upper flanks and summit of the volcano will be ~390, 500 and 650 m, respectively. These thicknesses represent ~13 to 22% of a 3 km thick ice layer.

The inverse relationship between pyroclast layer thickness and amount of ice loss shown in Table 3 implies that repetitive deposition of ash layers thinner than about 0.1 m could ultimately induce enough heating of underlying ice to completely remove a 3 km thick layer during the 50 ka period of non-accumulation. In practice there is no reason why eruptions should be equally spaced in time or should each produce exactly the same ash layer thickness. Also, re-working of ash deposits by the wind can lead to significant dune development on Mars (Parteli and Herrmann, 2007) so that layers might not be of uniform thickness, though deposition of ice in pore spaces as molecules migrate may act to stabilize ash layers on the upper flanks of volcanoes. Nevertheless, these illustrations gives an impression of the possible significant consequences of repeated eruptions producing thin pyroclast deposits during a period of no ice deposition.

4.3. Thick pyroclast deposits responding to annual and longer-term temperature changes

As noted earlier, pyroclast deposits with thicknesses in the 2 to 30 m range will transmit temperature changes to underlying ice on a martian annual timescale. These deposits are predicted to be present at between ~30 and ~200 km from vents in the case of 100 km^3 eruptions and at between ~150 and ~800 km for rare 1000 km^3 eruptions. The ~30 and ~200 km range of 2–30 m thick deposits from common 100 km^3 eruptions would cover most of the flanks of all large shield volcanoes. Furthermore, this distance range encompasses the full extent of the current glacial deposits identified on the north-west flanks of the Tharsis Montes (Head and Marchant, 2003; Shean et al., 2005, 2007; Kadish et al., 2008)). Thus these glacial deposits could potentially have been subjected to modifications on a martian annual timescale after any significant explosive eruption.

However, the temperature excursion driving these modifications would be the seasonal variation of the diurnal average temperature, not the hour-to-hour temperature that can be transmitted through thinner deposits. The diurnal average temperature on Mars currently varies as a function of season from ~205 to ~230 K at the equator and from ~140 to ~220 K at the poles (Kieffer et al., 1977). Thus nowhere is it likely that pyroclast deposits with thicknesses greater than a few meters would currently lead to loss of underlying ice. Simulations of the changes in the global temperature distribution due to the ~100 ka, 2 Ma and 15 Ma obliquity and eccentricity changes (e.g., Laskar et al., 2004) suggest that the same is true on longer time scales: although temperatures at the surface may exceed values that would cause significant ice evaporation at some time during the sol at low latitudes, the seasonal and longer-term variations in the diurnal mean temperatures that would be transmitted through pyroclast deposits more than a few meters thick would not be capable of causing significant loss of underlying ice.

This same argument applies to the even thicker pyroclast deposits predicted to be possible on volcano summits and upper flanks as a result of 100 km^3 eruptions and at all locations on volcanoes as a result of 1000 km^3 eruptions (see Fig. 3). The only consequence of such events is the preservation of underlying ice deposits.

5. Physical consequences of pyroclast deposition on glaciers

A typical 100 km^3 eruption will deposit several meters of ash on the upper and middle volcano flanks at the range of distances where glacial deposits are inferred to have been located on the Tharsis volcanoes (e.g., Head and Marchant, 2003). Such eruptions occur at ~1000 year intervals during each 1 Ma active phase of the volcano. Fifty such eruptions might occur during the ~50 ka half of the 100 ka time scale on which a glacier was growing. If each eruption deposited 5 m of ash (see Fig. 3), the total added would be an equivalent thickness of (50×5 m=) 250 m of pyroclasts. Given that the estimates of the current thicknesses of the glacial deposits are 2 to 3 km, it is clear that the silicate load of the glacier could easily be ~8–12%. If a rare 1000 km^3 eruptive event should chance to happen during

the ice accretion period, an additional 30 m of ash could be added. The possibility that ~10% of a volcano-covering glacier may consist of pyroclasts may help to account for the common presence of extensive systems of drop moraines and sublimation till deposits identified in areas where the ice has retreated (e.g., Head and Marchant, 2003; Shean et al., 2005, 2007; Kadish et al., 2008).

An additional effect of the presence of layers of pyroclasts within glacial ice may be the modification of the rheological properties of the glacier. Glaciers on the flanks of martian shield volcanoes have cold bases (e.g., Head and Marchant, 2003) and glacial advance is accomplished by internal shear. The shearing force is the component of the glacier weight parallel to the slope and hence is a function of the glacier density. Loosely packed (say 35% void space) low-vesicularity mafic pyroclasts will have a density of ~2000 kg m^{-3}, twice that of the ice above and below, potentially increasing glacial advance rates over what might otherwise be expected. Further, cold, unwelded pyroclast layers may represent zones of low resistance to shear stress. However, exploration of the consequences of these issues is beyond the scope of this paper.

6. Effects of pyroclastic density currents

It is common on Earth for large-volume silicic eruptions involving caldera collapse to produce not fall deposits but instead pyroclastic density currents, the final products of which are the deposits called ignimbrites. The largest of such deposits on Earth extend to many tens of km from the vent (Druitt, 1998). Mafic pyroclastic density currents are rare on Earth, but the greater degree of magma fragmentation expected in mafic explosive eruptions on Mars implies that mafic ignimbrites should be more common, and could be emplaced with temperatures of up to ~700 K (Wilson and Head, 1994). An explosive eruption from a 30 km diameter magma reservoir on Mars causing 1 km of vertical caldera collapse would release ~700 km^3 of magma. Pyroclastic density currents on Mars are able to travel to greater distances than on Earth mainly because the greater expansion of released magmatic gas in the martian environment produces initial eruption speeds ~2.5 times greater than those on Earth (Wilson and Head, 1994). If such a current were to spread radially from a summit vent for 300 km (at the upper end of the plausible range of distances for martian conditions - Wilson and Head, 1994) it could produce a deposit ~2.5 m thick on top of an existing glacial ice layer. Wilson and Head (2007b) show that about half of the heat content of a mafic lava flow deposit overlying ice would be transferred to the underlying ice, and that this could melt an ice thickness approximately equal to 5 times the thickness of the mafic layer. In the case of a mafic deposit overlying ice on Mars an allowance must be made for the fact that to melt the ice it must first be warmed up from a typical temperature of 210 K to the melting point at ~273 K, requiring about 1.3×10^5 J kg^{-1} of heat in addition to the 3.35×10^5 J kg^{-1} needed to melt the ice. Thus the ratio of melted ice thickness to deposit thickness is reduced from ~5 to ~3.6, so that in the case of a 2.5 m deposit thickness about 9 m depth of ice would be melted. This is only a very small fraction of the ~2–3 km estimated maximum thickness of cold-based glaciers on the Tharsis Montes. If a pyroclastic density current were channeled by summit topography so that it spread only onto a sector of the volcano flanks instead of radially, then all of these depth and thickness estimates might be increased by a factor of up to 10, but even 90 m of melting would not represent a significant fraction of a 3 km thick glacier. However, after, and indeed before, it had completely cooled, the ignimbrite sheet would begin to influence the temperature of surviving ice beneath it in the same way as the fall deposits considered earlier. The same arguments as to its effectiveness would apply, with a layer less than a few meters thick possibly having a strong influence on the amount of ice melted over a long period. Overall, we infer that the consequences of the deposition of deposits from explosive eruptions are similar, irrespective of whether the eruptions produce fall or flow deposits.

7. Summary

1) Estimates of the amounts of magma erupted from magma chambers of the sizes observed on large shield volcanoes imply that the thicknesses of fall deposits produced by explosive eruptions may range from a few to many hundreds of meters in summit areas and from a few to a few tens of meters on the volcano flanks.
2) Fall deposits may commonly be 0.1 m thick at 1000 km distance from source and the largest eruptions can produce millimeter-thick layers half way around the planet.
3) Volcanic deposits act to reduce evaporation of ice by providing a tortuous pathway to the atmosphere but may cause increased ice loss if the low albedo of the deposit causes surface warming that is communicated by conduction to underlying ice.
4) In practice, thin (<~2 m thick) deposits able to transmit diurnal surface temperature variations to underlying ice are the only ones capable of causing net ice loss. However, these deposits may have a major effect on polar water ice because of the low seasonal water ice deposition rates. Such deposits may also cause significant thinning of glacial deposits on the flanks of low-latitude volcanoes during periods when no net deposition of ice is taking place.
5) Thick (>a few meters) volcanic deposits, however they are emplaced, always act to preserve underlying ice deposits.
6) Deposits from pyroclastic density currents (ignimbrites) emplaced onto ice may cause initial melting of a depth of ice up to 3.6 times the thickness of the volcanic deposit as they cool, but subsequently will act to preserve the remaining ice.
7) Loading of glacial ice deposits by layers of volcanic tephra will in general increase the shear stress within the glacier, thus increasing advance rates even in cold-based glaciers.

Acknowledgements

This work was supported in part by grants to JWH from the NASA Mars Express High Resolution Stereo Camera Co-Investigator Program (JPL 1237163) and the Mars Data Analysis Program (NNX07AN95G and NNG05GQ46G). We thank David Marchant, James Rice and Benjamin Edwards for very helpful reviews.

References

Blake, S., 1981. Volcanism and the dynamics of open magma chambers. Nature 289, 783–785.
Boynton, W.V., 24 others, 2002. Distribution of hydrogen in the near-surface of Mars: evidence for sub-surface ice deposits. Science 297, 81–85.
Cabrol, N.A., 2006. Sedimentology of home plate at Gusev Crater. Mars. Eos Transactions American Geophysical Union. Fall Meeting Supplement, Abstract P44A-06, vol. 87 (52).
Carey, S., Sparks, R.S.J., 1986. Quantitative models of fallout and dispersal of tephra from volcanic eruption columns. Bulletin of Volcanology 48, 109–125.
Carslaw, H.S., Jaeger, J.C., 1947. Conduction of heat in solids. Oxford Univ. Press, Oxford, U.K. 386 pp.
Dickson, J.L., Head, J.W., Marchant, D.R., 2008. Late Amazonian glaciation at the dichotomy boundary on Mars: evidence for glacial thickness maxima and multiple glacial phases. Geology 36 (5), 411–414.
Druitt, T., 1998. Pyroclastic density currents. In: Gilbert, J.S., Sparks, R.S.J. (Eds.), The Physics of Explosive Volcanic Eruptions. Special Publications, vol. 145. Geological Society, London, pp. 145–182.
Edgett, E.S., Butler, B.J., Zimbelman, J.R., Hamilton, V.E., 1997. Geologic context of the Mars radar "stealth" region southwestern Tharsis. Journal of Geophysical Research 102, 21545–21567.
Elphic, R.C., Feldman, W.C., Prettyman, T.H., Tokar, R.L., Lanza, N., Lawrence, D.J., Head, J.W., Mischna, M.A., Richardson, M.I., 2004. Enhanced water-equivalent hydrogen on the western flanks of the Tharsis Montes and Olympus Mons: remnant subsurface ice or hydrate minerals. Lunar and Planetary Science XXXV: abstract no. 2011.
Fanale, F.P., Salvail, J.R., 1984. An idealized short-period comet model; surface insolation, H_2O flux, dust flux, and mantle evolution. Icarus 60, 476–511.
Fanale, F.P., Salvail, J.R., 1990. Evolution of the water regime of Phobos. Icarus 88, 380–395.
Farrand, W.H., Singer, R.B., 1992. Alteration of hydrovolcanic basaltic ash: observations with visible and near-infrared spectrometry. Journal of Geophysical Research 97 (B12), 17,393–17,408.

Glaze, L., Baloga, S.M., 2002. Volcanic plume heights on Mars: limits of validity for convective models. Journal of Geophysical Research 107 (E10). doi:10.1029/2001JE001830.
Grassi, D., Fiorenza, C., Zasova, L.V., Ignatiev, N.I., Maturilli, A., Formisano, V., Giuranna, M., 2005. The martian atmosphere above great volcanoes: early planetary Fourier spectrometer observations. Planetary and Space Science 53, 1053–1064.
Haberle, R.M., McKay, C.P., Schaeffer, J., Cabrol, N.A., Grin, E.A., Zent, A.P., Quinn, R., 2001. On the possibility of liquid water on present-day Mars. Journal of Geophysical Research 106, 23317–23326.
Head, J.W., Wilson, L., 1998. Tharsis Montes as stratovolcanoes?: 1. The role of explosive volcanism in edifice construction and implications for the volatile contents of edifice-forming magmas. Lunar and Planetary Science XXIX, Abstract no. 1127. Lunar and Planetary Institute, Texas.
Head, J.W., Marchant, D.R., 2003. Cold-based mountain glaciers on Mars: Western Arsia Mons. Geology 3 (7), 641–644.
Head, J.W., Marchant, D.R., Agnew, M.C., Fassett, C.I., Kreslavsky, M.A., 2006a. Extensive valley glacier deposits in the northern mid-latitudes of Mars: evidence for Late Amazonian obliquity-driven climate change. Earth and Planetary Science Letters 241, 663–671. doi:10.1016/j.epsl.2005.11.016.
Head, J.W., Nahm, A.L., Marchant, D.R., Neukum, G., 2006b. Modification of the dichotomy boundary on Mars by Amazonian mid-latitude regional glaciation. Geophysical Research Letters 33, L08S03. doi:10.1029/2005GL024360.
Hodges, C.A., Moore, H.J., 1994. Atlas of volcanic landforms on Mars, U. S. Geological Survey Professional Paper 1534.
James, P.B., Bonev, B.P., Wolff, M.J., 2005. Visible albedo of Mars south polar cap: 2003 HST observations. Icarus 174 (2), 596–599.
Kadish, S.J., Head, J.W., Parsons, R.L., Marchant, D.R., 2008. The Ascraeus Mons fan-shaped deposit: Volcano-ice interactions and the climatic implications of cold-based tropical mountain glaciation. Icarus 197 (1), 84–109.
Kerber, L., Head, J.W., Madeleine, J.B., Wilson, L., Forget, F., 2008. Modeling ash dispersal from Apollinaris Patera: implications for the Medusae Fossae formation. Lunar and Planetary Science XXXIX, Abstract no. 1881. Lunar and Planetary Institute, Houston, Texas.
Kieffer, H.H., Titus, T.N., 2001. TES mapping of Mars' north seasonal cap. Icarus 154 (1), 162–180.
Kieffer, H.H., Chase, S.C., Miner, E.D., Palluconi, F.D., Munch, G., Neugebauer, G., Martin, T.Z., 1976a. Infrared thermal mapping of the Martian surface and atmosphereL first results. Science 193, 780–785.
Kieffer, H.H., Christensen, P.R., Martin, T.Z., Miner, E.D., Palluconi, F.D., 1976b. Temperatures of the martian surface and atmosphere: Viking observation of diurnal and geometric variations. Science 194, 1346–1351.
Kieffer, H.H., Martin, T.Z., Peterfreund, A., Jakosky, B., Miner, E.D., Palluconi, F.D., 1977. Thermal and albedo mapping of Mars during the Viking primary mission. Journal of Geophysical Research 82, 4249–4291.
Laskar, J., Levrard, B., Mustard, J.F., 2002. Orbital forcing of the martian polar layered deposits. Nature 419, 375–377. doi:10.1038/nature01066.
Laskar, J., Correia, A.C.M., Gastineau, M., Joutel, F., Levrard, B., Robutel, P., 2004. Long term evolution and chaotic diffusion of the insolation quantities of Mars. Icarus 170, 343–364.
Latham, J.-P., Munjiza, A., Lu, Y., 2002. On the prediction of void porosity and packing of rock particulates. Powder Technology 125 (1), 10–27.
Mellon, M.T., Fekdman, W.C., Prettyman, T.H., 2004. The presence and stability of ground ice in the southern hemisphere of Mars. Icarus 169 (2), 324–340.
Milkovich, S.M., Head, J.W., Marchant, D.R., 2006. Debris-covered piedmont glacier deposits along the northwest flank of the Olympus Mons scarp: evidence for low-latitude ice accumulation during the Late Amazonian of Mars. Icarus 181, 388–407. doi:10.1016/j.icarus.2005.12.006.
Morton, B.R., Taylor, G.I., Turner, J.S., 1956. Turbulent gravitational convection from maintained and instantaneous sources. Philosophical Transactions of the Royal Society of London A 234, 1–23.
Moudden, Y., McConnell, J.C., 2005. A new model for multiscale modeling of the Martian atmosphere, GM3. Journal of Geophysical Research 110, E04001. doi:10.1029/2004JE002354.
Mouginis-Mark, P.J., Wilson, L., Head, J.W., 1982. Explosive volcanism on Hecates Tholus, Mars: investigation of eruption conditions. Journal of Geophysical Research 87, 9890–9904.
Mouginis-Mark, P.J., Wilson, L., Zimbelman, J.R., 1988. Polygenic eruptions on Alba Patera, Mars. Bulletin of Volcanology 50, 361–379.
Neukum, G., Jaumann, R., Hoffman, H., Hauber, E., Head, J.W., Basilevsky, A.T., Ivanov, B.A., Werner, S.C., van Gasselt, S., Murray, J.B., McCord, T., HRSC Team, 2004. Recent and episodic volcanic and glacial activity on Mars revealed by the High Resolution Stereo Camera. Nature 432, 971–979.
Parteli, E.J.R., Herrmann, H.J., 2007. Dune formation on the present Mars. Physical Review E 76 (4), 041307. doi:10.1103/PhysRevE.76.041307.
Phillips, R.J., Seu, R., Biccari, D., Campbell, B.A., Plaut, J.J., Zuber, M.T., Murchie, S., Byrne, S., Safaeinili, A., Orosei, R., Marinangeli, L., Masdea, A., Picardi, G., Smrekar, S.E., Carter, L.M., Putzig, N.E., Nunes, D.C., SHARAD Team, 2007. North polar deposits on Mars: new insights from MARSIS, SHARAD and other MRO instruments. Lunar and Planetary Science XXXVIII, Abstract no. 1925, Lunar and Planetary Institute, Houston, Texas.
Rice, J.W., Farrand, W., McCoy, T., Schmidt, M., Yingst, R.A., ATHENA team, 2006. Origin of Home Plate, Columbia Hills, Mars: Hydrovolcanic hypothesis. Eos Transactions American Geophysical Union, vol. 87(52). Fall Meeting Supplement, Abstract P41B-1274.
Schaber, G.G., Horstman, K.C., Dial, A.L., 1978. Lava flow materials in the Tharsis region of Mars. Proceedings of the Lunar and Planetary Science Conference, 9th 33,433–34,458.
Scott, E.D., Wilson, L., 2000. Cyclical summit collapse events at Ascraeus Mons, Mars. Journal of the Geological Society of London 157, 1101–1106.
Shean, D.E., Head, J.W., Marchant, D.R., 2005. Origin and evolution of a cold-based tropical mountain glacier on Mars: the Pavonis Mons fan-shaped deposit. Journal of Geophysical Research 110, E05001. doi:10.1029/2004JE002360.
Shean, D.E., Head, J.W., Fastook, J.L., Marchant, D.R., 2007. Recent glaciation at high elevations on Arsia Mons, Mars: implications for the formation and evolution of large tropical mountain glaciers. Journal of Geophysical Research 112, E03004. doi:10.1029/2006JE002761.
Smith, D.E., Zuber, M.T., Solomon, S.C., Phillips, R.J., Head, J.W., Garvin, J.B., Banerdt, W.B., Muhleman, D.O., Pettengill, G.H., Neumann, G.A., Lemoine, F.G., Abshire, J.B., Aharonson, O., Brown, C.D., Hauck, S.A., Ivanov, A.B., McGovern, P.J., Zwally, H.J., Duxbury, T.C., 1999. The global topography of Mars and implications for surface evolution. Science 284 (5422), 1932.
Sparks, R.S.J., 1978. The dynamics of bubble formation and growth in magmas: a review and analysis. Journal of Volcanology and Geothermal Research 3, 1–37.
Sparks, R.S.J., 1986. The dimensions and dynamics of volcanic eruption columns. Bulletin of Volcanology 48, 3–15.
Turner, R., Hurst, T., 2001. Factors influencing volcanic ash dispersal from the 1995 and 1996 eruptions of Mount Ruapehu, New Zealand. Journal of Applied Meteorology 40 (1), 56–69.
Wallace, D., Sagan, C., 1979. Evaporation of ice in planetary atmospheres: ice-covered rivers on Mars. Icarus 39, 385–400.
Weitz, C.M., Head, J.W., Pieters, C.M., 1998. Lunar regional dark mantle deposits: Geologic, multipsectral, and modeling studies. Journal of Geophysical Research, 103, 22725–22759.
Wilson, L., 1999. Explosive Volcanic Eruptions — X. The influence of pyroclast size distributions and released magma gas contents on the eruption velocities of pyroclasts and gas in Hawaiian and plinian eruptions. Geophysical Journal International 136, 609–619.
Wilson, L., Walker, G.P.L., 1987. Explosive volcanic eruptions — VI. Ejecta dispersal in plinian eruptions: the control of eruption conditions and atmospheric properties. Geophysical Journal of the Royal Astronomical Society 89, 657–679.
Wilson, L., Head, J.W., 1994. Mars: review and analysis of volcanic eruption theory and relationships to observed landforms. Reviews of Geophysics 32, 221–264.
Wilson, L., Head, J.W., 2007a. Explosive volcanic eruptions on Mars: tephra and accretionary lapilli formation, dispersal and recognition in the geologic record. Journal of Volcanology and Geothermal Research 163, 83–97.
Wilson, L., Head, J.W., 2007b. Heat transfer in volcano–ice interactions on Earth. Annals of Glaciology 45, 83–86.
Wilson, L., Sparks, R.S.J., Huang, T.-C., Watkins, N.D., 1978. The control of volcanic column heights by eruption energetics and dynamics. Journal of Geophysical Research 83, 1829–1836.
Wilson, L., Head, J.W., Mitchell, K.L., 1998. Tharsis Montes as stratovolcanoes?: 2. Lines of evidence for explosive volcanism in far-field deposits. Lunar and Planetary Science XXIX, Abstract no. 1125. Lunar and Planetary Institute, Houston, Texas.
Wilson, L., Scott, E.D., Head, J.W., 2001. Evidence for episodicity in the magma supply to the large Tharsis volcanoes. Journal of Geophysical Research 106 (E1), 1423–1433.